Experimental investigation of bifurcations in a thermoacoustic engine

Vishnu R. Unni[1 2], Yogesh Prasaad M. S. [2], N. T. Ravi[2], S. Md. Iqbal[2], Bala Pesala[2], and R. I. Sujith*[1]

[1]*Department of Aerospace Engineering, Indian Institute of Technology Madras Chennai-600036, India*

[2]*Central Electronics Engineering Research Institute, Council of Scientific and Industrial Research Chennai-6000113, India*

(Submission date: September 03, 2013; Revised Submission date: May 08, 2014; Accepted date: August 18, 2014)

ABSTRACT

In this study, variation in the characteristics of the pressure oscillations in a thermoacoustic engine is explored as the input heat flux is varied. A bifurcation diagram is plotted to study the variation in the qualitative behavior of the acoustic oscillations as the input heat flux changes. At a critical input heat flux (60 Watt), the engine begins to produce acoustic oscillations in its fundamental longitudinal mode. As the input heat flux is increased, incommensurate frequencies appear in the power spectrum. The simultaneous presence of incommensurate frequencies results in quasiperiodic oscillations. On further increase of heat flux, the fundamental mode disappears and second mode oscillations are observed. These bifurcations in the characteristics of the pressure oscillations are the result of nonlinear interaction between multiple modes present in the thermoacoustic engine. Hysteresis in the bifurcation diagram suggests that the bifurcation is subcritical. Further, the qualitative analysis of different dynamic regimes is performed using nonlinear time series analysis. The physical reason for the observed nonlinear behavior is discussed. Suggestions to avert the variations in qualitative behavior of the pressure oscillations in thermoacoustic engines are also provided.

1. INTRODUCTION

A thermoacoustic engine (TAE) is a device that can produce high amplitude acoustic oscillations from thermal energy. The pressure oscillations produced by a TAE can have amplitudes of the order of 180 dB [1]. With a suitably designed transducer such as a linear alternator, the acoustic energy from these pressure oscillations can be converted to electrical energy [1]. Thermoacoustic engine coupled with such a transducer is called a thermoacoustic generator (TAG). Various types of thermoacoustic generators have been designed in the past [2] [3]. The unique feature of a thermoacoustic generator is that it can produce electricity

Prof. Wolfgang Polifke served as the sole independent editor for this article

*Corresponding author: sujith@iitm.ac.in and vishnu r unni [vishnu.runni@gmail.com]

from various heat sources. This quality makes it capable of being a hybrid power generation solution which can be operated using heat from the sun and biomass.

However, the amount of heat that can be supplied by these sources varies over time. From our experiments, it was observed that the characteristics of oscillations in a thermoacoustic engine change as the input heat flux is varied. When the oscillatory characteristics of thermoacoustic engine change, the transduction (acoustic energy to electrical energy) process gets affected. Linear alternators used in a thermoacoustic generator in order to convert acoustic energy to electrical energy are designed to be most efficient at a particular frequency (i.e., at its natural frequency) [1, 4–6]. Hence, even a slight variation of the operational frequency from the design frequency can cause a drastic drop in transduction efficiency. This implies that the variation in the oscillation frequency of TAE with input heat flux will cause reduction in the overall efficiency of the thermoacoustic generator. Hence, an understanding of the nonlinear phenomena that cause variations in the characteristics of pressure oscillations in a TAE is essential in order to explore new control and design strategies to improve the efficiency of a TAG.

Nonlinear behavior of various thermoacoustic devices have been studied extensively in the past. Yazaki et al. [7] studied the dynamics of spontaneous acoustic oscillations generated in a stainless steel tube in the presence of a steep thermal gradient (Taconis oscillations). It was observed in their experiments that simultaneous presence of multiple incommensurate frequencies in Taconis oscillations resulted in various nonlinear phenomena. The different dynamics observed in the experiments were analyzed using the methods from the theory of nonlinear dynamical systems such as reconstruction of phase space and analysis of Poincaré section and was classified as quasiperiodicity, frequency locking and onset of chaos. Nonlinear acoustic oscillations have been observed in thermoacoustic systems involving combustion. Dynamics of combustion driven oscillations for a ducted laminar premixed flame at different operational conditions was studied by Kabiraj et al. [8]. In their experiments, they were able to observe nonlinear behaviors such as quasiperiodicity, frequency locking, intermittency and chaos. They analyzed oscillations at different dynamic regimes using tools from nonlinear time series analysis. Further, they performed a detailed classification of different dynamic regimes through a bifurcation study.

In a standing wave thermoacoustic engine, nonlinear behavior of acoustic oscillations was first observed by Swift et al. [1]. During the starting of a TAE coupled with a thermoacoustic refrigerator, for a fixed input heat flux, they observed that the acoustic oscillations in TAE were produced and quenched in alternate cycles with a period of one hour. However, at steady state, stable limit cycle oscillations were observed. Atchley et al. [9] observed that in a standing wave thermoacoustic engine, presence of one mode can affect the stability of the other mode. This interaction was in turn found to result in modulated acoustic pressure oscillations resembling beats. Atchley et al. [9] attributed this beat like behavior to quasiperiodicity. However, a rigorous time series analysis was not performed in order to analyze these nonlinear oscillations. In our investigation, we perform nonlinear time series analysis in order to explore the qualitative nature of the observed nonlinear phenomena and there by confirm the existence of quasiperiodic regime in the oscillatory characteristics of a standing wave thermoacoustic engine.

Apart from standing wave thermoacoustic engines, traveling wave thermoacoustic engines are also found to exhibit nonlinear oscillatory behaviors. Recently, Yu et al. [10] reported a nonlinear oscillatory phenomena occurring during the start-up of a traveling wave looped-tube thermoacoustic engine. It was observed that a fishbone-like instability existed during the start-up of the engine. In another investigation performed by Yu et al. [11] two modes with widely different stabilities were observed to get induced in a looped-tube traveling wave thermoacoustic engine. Among the two modes, the stability of the high frequency mode (HFM) was found to be affected by the presence of low frequency mode (LFM). Furthermore, quasiperiodic oscillations were observed during the transition of oscillations from HFM to LFM. Likewise, in the experiments conducted by Biwa et al. [12] in a looped-tube traveling wave thermoacoustic engine, the transition from standing wave mode to travelling wave mode was observed to occur through a quasiperiodic transition state. In this paper, we report the observed interaction of multiple modes of acoustic oscillations in a standing wave thermoacoustic engine resulting in various interesting dynamics.

There are only a few theoretical investigations that concentrate on the nonlinear characteristics of acoustic oscillations TAE. Considering the various nonlinear mechanisms involved in the operation of a TAE, a two port network model and start up criteria for thermoacoustic engines was proposed by Hu et al. [13]. The proposed startup criteria, based on the Nyquist stability criteria was able to predict the effects of the engine configuration and operational parameters on the onset mode. Yuan et al. [14] suggested a quasi-one dimensional model for a thermoacoustic engine incorporating the nonlinear effects. This model was able to reproduce experimental observations of the nonlinear oscillations in a TAE by Atchely et al. [9] to a large extend.

Theoretical models that incorporate the nonlinearities can help improve the design procedure for a thermoacoustic engine. However, detailed experimental observations are required to understand various nonlinear phenomena involved in the operation a TAE. Further, variation in the oscillatory behavior of a thermoacoustic engine can have deteriorating effects on the efficiency of a TAG. Hence, it is essential to study these nonlinear acoustic oscillations present in a TAE in detail in order to be able to tailor the behavior of a TAE to ensure maximum performance for a practical thermoacoustic generator. Keeping these goals in mind, in the current work, we investigate the variation in characteristics of the steady state acoustic oscillations in a standing wave thermoacoustic engine through a bifurcation study. From our experiments, we observe a series of bifurcations in the qualitative behavior of a thermoacoustic engine as the input heat flux to the system is varied. Further, we focus on exploring the qualitative nature of the different dynamic regimes observed in the bifurcation study using the tools from nonlinear time series analysis. Subsequently, using the results from nonlinear time series analysis, we explain the reason for the observed bifurcations. With this new understanding, we also suggest some design strategies that can be employed to improve the performance of a practical TAG. We hope that the experimental observations and their detailed analysis reported in this investigation can contribute to a better understanding of the nonlinear behavior of TAE and there by improve the design strategy of a TAE.

2. EXPERIMENTAL SETUP

The thermoacoustic engine setup used for the present study has a standing wave design. The parameters used to design the thermoacoustic engine were optimized using the optimization platform called DELTA EC [15]. The schematic diagram of the TAE is shown in Fig. 1. It consists of a stack sandwiched between two heat exchangers. This assembly is then inserted into a resonator. The stack is a ceramic monolithic structure (Corning Celcore substrate, Cordierite). It has pores of square cross section and a pore density of 900 square cells per square inch. The wall thickness of the stack is 0.0635 mm. The resonator is divided into two parts:a hot duct and a cold duct. Both the ducts are joined together on either sides of the cold heat exchanger to form one single duct of a uniform cross section (50 $mm \times 50\ mm$). The resonator assembly has a total length of 500 mm. One end of the duct (hot side) is closed and other end (cold side) is partially open (this opening is provided such that a linear alternator can be connected to the thermoacoustic engine and electricity can be produced). The cold heat exchanger is made of copper tubes that will transport cold water in and out of the system. The hot heat exchanger is fabricated by winding a Nichrome wire around a square shell made of Cynthanium sheet. The wire used for the particular experiment is of gauge 30 and has a resistance of 21 Ω. A variable voltage power supply (Dimmerstat) is used to power the heater. A refrigerator capable of maintaining a temperature of $5°C$, for a mass flow rate of 10 LPM is used to circulate water through the cold heat exchanger. For the bifurcation analysis reported in this paper, the cold side temperature was maintained at $6 \pm 2°C$. The stack length to the resonator length ratio (λ_s) is 0.08. Fluctuating pressure inside the duct was measured by the piezoelectric transducers (Model No: 103B02 PCB Peizotronics) mounted on the side walls of the TAE as shown in Fig. 1. Uncertainty in

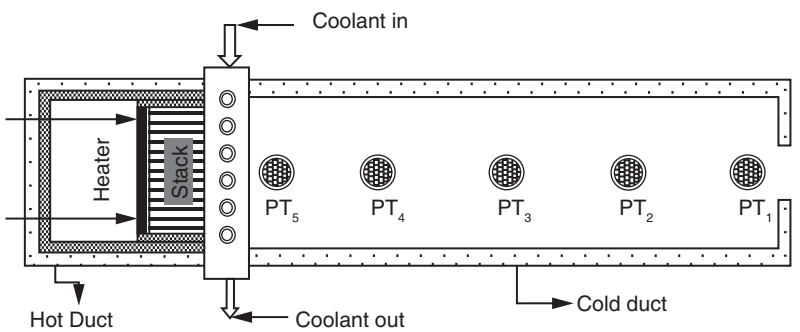

Figure 1: Schematic diagram of the thermoacoustic engine. The stack is sandwiched between the cold and the hot heat exchangers. PT_{1-5} are pressure transducers (Model No: 103B02 PCB Peizotronics) used to measure the acoustic pressure at different locations. All the analysis in this paper is performed using the pressure readings from the transducer PT_1. Hot heat exchanger is heated by passing current through Nichrome wire. The stack length to the resonator length ratio (λ_s) is 0.08.

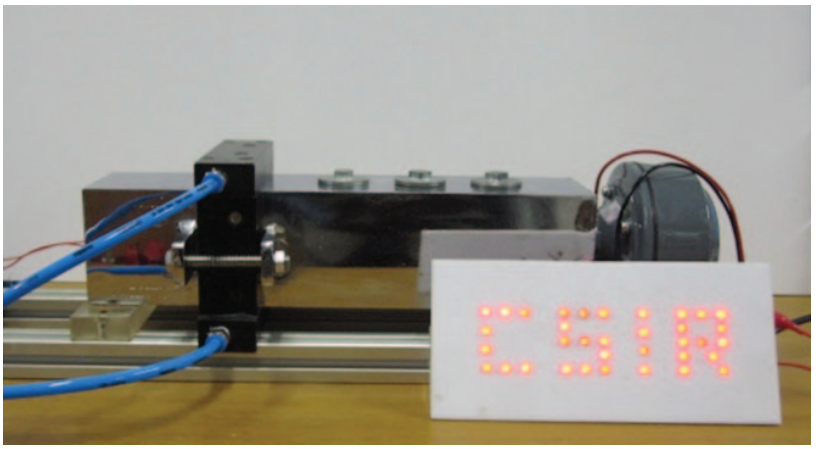

Figure 2: The prototype thermoacoustic engine powering an LED display. The electrical power output of the thermoacoustic engine is 3 Watts for an input heat flux of 200 Watts.

pressure measurements is 0.14 *Pa* (0.02 mpsi). In order to quantify acoustic damping of the system, acoustic decay rate of the engine was estimated. Under cold flow conditions, for a frequency of 500 *Hz*, the decay rate was measured to be 27/*s*. Measurement of acoustic decay rate was done in the following manner. The engine was exited using a 500 *Hz* acoustic signal produced by a speaker positioned at the partiallly open end. Further, the excitation is stopped abruptly. Decay of the acoustic oscillations within the thermoacoustic engine on removal of the external exitation is recorded using a pressure transducer attached to the engine. The exponential decay rate of the amplitude of acoustic oscillations can be estimated from the recorded data by evaluating the envelop of the decaying pressure signal. This decay rate is representative of the acoustic damping in the system. In order to ensure the repeatability, experiments were conducted only if the acoustic decay rates were within $\pm$ 10% of the above value.

3. PHASE SPACE RECONSTRUCTION

The dynamics of a system can be understood by studying the evolution of the state point in the state space corresponding to the system. A state space is an *N* dimensional space, represented by *N* state variables independent of each other. These variables together will completely and uniquely define the state of the system (referred as state point) at a specified time [16–18]. The state space (also called phase space) contains all states that a dynamical system can possibly reach. Evolution of state point in phase space (represented in a phase plot) will help us understand the complex dynamics of the systems. Dynamics of systems with three or less degrees of freedom is very easy to visualize in a phase space plot. In order to visualize the dynamics of systems with higher degrees of freedom, projections of state space in two or three dimensions can

be used [19, 20]. The number of dimensions of the phase space is an indication of the complexity of the system. A state represented in the phase space can evolve only in one possible direction in time. Hence, if the evolution equation for the system is available we can reconstruct the complete state space evolving from an initial state point. But in the case of the TAE, an evolution equation that represents its complex dynamics is not at our disposal in order to reconstruct the phase space from a given initial condition. Hence, some indirect methods are followed to reconstruct the phase space for TAE.

Takens, in his embedding theorem [17] suggests that the state space can be reconstructed from time delayed vectors that can be extracted from the time series data of any one state variable obtained experimentally. The two parameters that are of prime importance in reconstructing the state space are the following, the embedded dimension [16] and the optimal time delay [16]. Abarbanel [16] in detail has described how state space reconstruction can be done for an experimental data. Further, Kabiraj et. al. [8] has demonstrated use of these techniques in identifying the dynamical states of a thermoacoustic system.

Embedded dimension is the estimated phase space dimension of a system [16]. An appropriate embedded dimension is required to capture the dynamics of the system in a state space created by the time delay vectors with no ambiguity. With appropriate embedded dimensions, the state point can evolve only in one direction at any time. Hence in theory, the path lines of the state point never intersect with each other. However, the path lines of the phase space constructed from the experimental data will not always follow this because of the presence of random errors in the system. In this work, the appropriate dimension for the phase space is estimated by using the false nearest neighbor method [16]. From analysis, it was found that the maximum embedded dimension for the TAE system under discussion is four. However, a three dimensional phase space was found to be sufficient to represent the attractor with clarity of its structure.

The optimal time delay (τ) used for representing the evolution of the state point in phase space should be large enough to perfectly capture the dynamics of the system but not too large that the delay vectors will be completely unrelated. It can be estimated in many ways. For linear systems, τ corresponding to the first zero crossing of the autocorrelation function is considered as the optimal time lag. The preferred method for a nonlinear system is the method of average mutual information [8, 16]. For all the results discussed in this paper, method of average mutual information is used to find the optimal time delay.

Once the embedded dimension and an optimal time delay are obtained, phase space can be reconstructed from the time series data of a state variable. In a particular dynamical system, consider $P(t)$ to be the time series data of one of the state variables of the system. If the phase space corresponding to that dynamical system is of three dimensions and τ is the optimal time delay, then the phase space can be reconstructed by plotting the time series vector $P(t)$ and the delay vectors $P(t + \tau)$ and $P(t + 2\tau)$ along the three axis of state space. In this paper, the time series data of pressure from the pressure transducer PT_1 is used to reconstruct the state space in three dimensions. The data is sampled at a rate of 40K Samples/s.

4. RESULTS AND DISCUSSIONS

Bifurcation analysis was performed on TAE in order to study the qualitative change in the thermoacoustic oscillations with varying input heat flux. In the present study, the input heat flux was varied from 0 to 250 Watts. A bifurcation diagram is plotted between local pressure maxima for the pressure time trace and the input heat flux (Fig. 3). Figure 3a shows the pressure values for increasing input heater power (forward direction) and Fig. 3b shows the pressure values for decreasing heater power (reverse direction). In the forward direction, the system starts to produce sound beyond a critical input heater power of 67 Watts. Here, the amplitude of the local maxima in each cycle of the pressure signal are equal, hence the system is in a limit cycle. The frequency of oscillations correspond to the fundamental frequency of the resonator for the given geometry, boundary conditions and the particular temperature gradient across the stack. As the

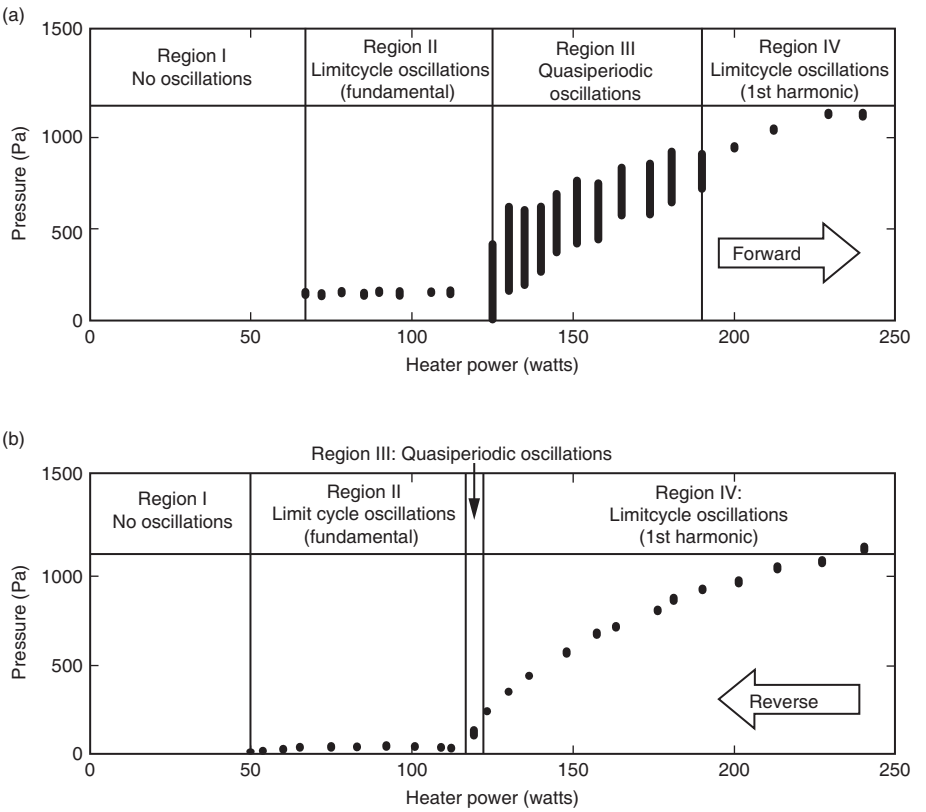

Figure 3: Bifurcation diagram. Local maxima of each cycle in the pressure signal are plotted for each heater power location. a) Increasing heat flux (Forward direction). b) Decreasing heat flux (Reverse direction). Comparing the forward and reverse path of the bifurcation diagram, it is evident that there is hysteresis in the bifurcation. This is indicative of a subcritical bifurcation.

heater power is increased, the system remains in limit cycle (region II). The normalized pressure trace (i.e., $P/max\ (|P|)$) for oscillations in region II is shown in Fig. 4. Here all the local maxima have the same amplitude. Hence we can see that in the bifurcation plot (Fig. 3) these state points correspond to only a single amplitude of pressure.

In FFT (Fig. 5) corresponding to pressure fluctuations in region II, we can see that the power is maximum for the fundamental frequency. Even though the presence of super harmonics is evident, their amplitude levels are not comparable with the

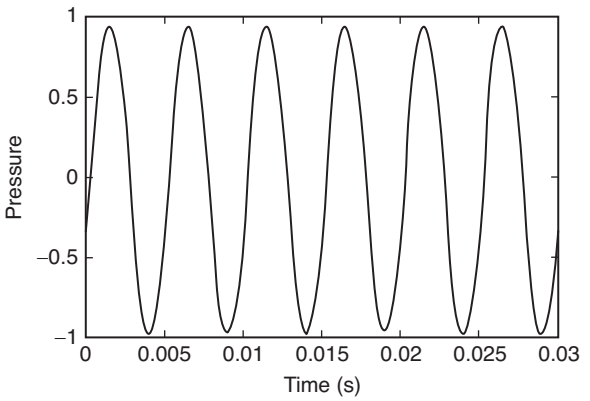

Figure 4: Time trace of acoustic pressure signal corresponding to limit cycle oscillations (region II of Fig. 3, fundamental mode) for an input heat flux of 72 Watts. Note that all the local maxima have same amplitude. Also, the pressure value is normalized.

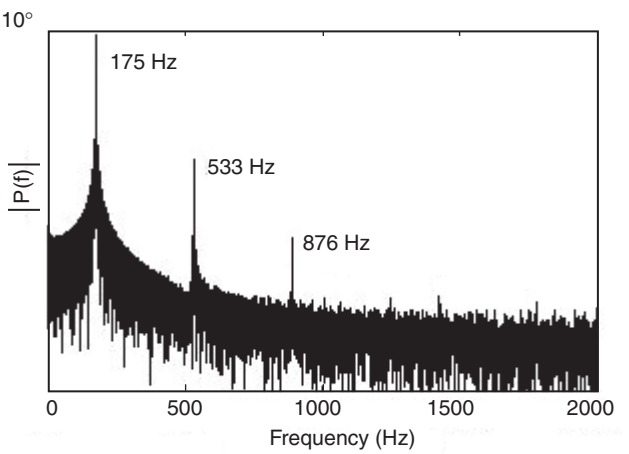

Figure 5: FFT corresponding to limit cycle oscillations (region II of Fig. 3, fundamental mode). Here, the input heat flux is 72 Watts.

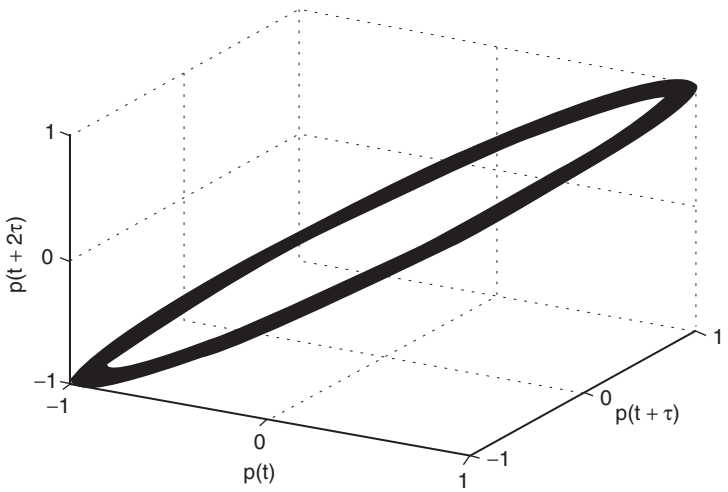

Figure 6: Phase portrait corresponding to limit cycle oscillations (region II of Fig. 3, fundamental mode). Here, the input heat flux is 72 Watts and the pressure value is normalized.

amplitude of the fundamental frequency. The frequency of oscillations in this region is found to increase with increase in heat flux (region II of Fig. 3). This behavior is the result of the increase in the temperature gradient across the length of stack with increasing input heat flux. As the temperature gradient increases, the local temperature of the working fluid inside the stack increases. This results in an increase in local speed of sound along the length of the stack. The temperature gradient along the stack alters the mode shape of the standing wave formed inside the resonator duct of the thermoacoustic engine in such a manner that it results in an increase in the oscillation frequency (note that for a duct with axilal temperature gradient, natural modes have frequency varying with the temperature gradient [21]). This shift in frequency is of the order of 10 to 30 Hz. Figure 6 is the phase portrait of the system for fundamental oscillations (region II). Here, the state point evolves to form a single loop in its phase space. This clearly indicates a limit cycle behavior.

On further increase in the heater power, the growth of second mode oscillation is observed. As the amplitude of the second mode oscillations becomes comparable to the amplitude of the fundamental mode, the dynamic behavior of the system changes. This is the second bifurcation. Here the oscillations exhibit a beat like behavior (region III in Fig. 3a). The local maxima in the pressure trace no longer have a constant amplitude (Fig. 7). FFT of the pressure signal has two frequencies (f1 and f2) with comparable amplitude. Further, f1 and f2 are incommensurate to each other (Fig. 8). Additional frequencies which are the linear combinations of the incommensurate frequencies (such as, f1 + f2) are also present in the power spectra. This is the characteristics of a quasiperiodic oscillation.

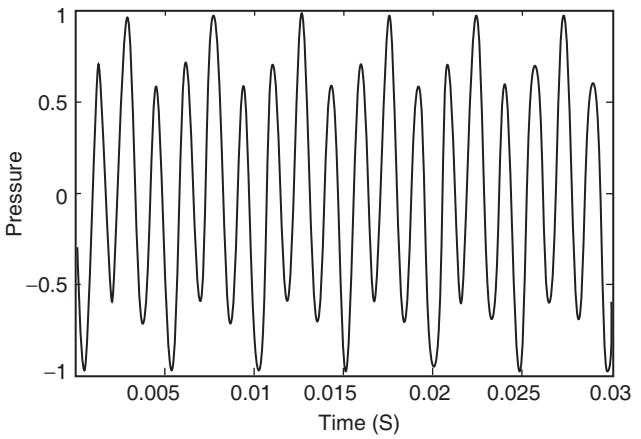

Figure 7: Time trace of acoustic pressure signal corresponding to quasiperiodic oscillations (region III of Fig. 3) for an input heat flux of 160 Watts. Note that the local maxima have different amplitude. Also, the pressure values are normalized.

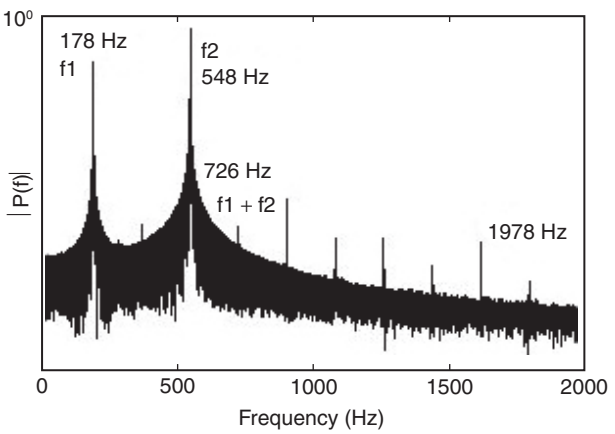

Figure 8: FFT corresponding to quasiperiodic oscillations (region III of Fig. 3). Here, the input heat flux is 160 Watts.

Quasiperiodicity is observed in a system if at least two frequencies present in the system are incommensurate. In such a case, the oscillations will become aperiodic and the trajectories of the state point in the phase space will not close on itself. This causes the state point to evolve on the surface of a torus (Fig. 9). Since there are two incommensurate frequencies in the present system, the attractor in this case is a 2-torus (a torous described by two circles) [18]. Transition from region II to region III is a

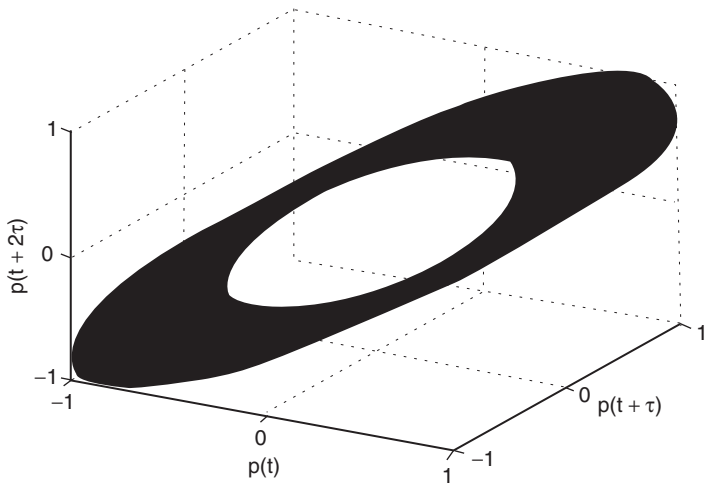

Figure 9: Phase portrait corresponding to quasiperiodic oscillations (region III of Fig. 3). Here, the input heat flux is 160 Watts and the pressure values are normalized.

bifurcation in the qualitative behavior of the system. This type of bifurcation, where stable limit cycle transitions to a quasiperiodic state is called Neimer-Saker bifurcation or secondary bifurcation.

The growth of higher modes of pressure oscillation and reduction of acoustic power in fundamental mode in region III can be explained as follows. In a standing wave thermoacoustic engine, the optimal pore size of the stack is 2 to 3 times the thermal penetration depth of the working fluid. Thermal penetration depth (δ_k) is the distance through which heat can be transferred in a time interval equal to the period of the oscillations divided by π.

$$\delta_k = \sqrt{\frac{2k}{\omega \rho C_P}} \tag{1}$$

Here, k is the thermal conductivity of the working fluid, C_p is its specific heat capacity at constant pressure and ω is the angular frequency of the oscillations. As the stack temperature increases at higher heat flux rates, the mean temperature of the working fluid surrounding the stack also increases. This increase in local temperature of working fluid causes an increase in the local thermal penetration depth of the fluid. Since the thermal penetration increases with input heat flux, at high input heat flux rates the pore size of the stack becomes non-optimal for the fundamental mode. Hence, the acoustic power of the fundamental mode reduces at high heat flux rates. However, thermal penetration length decreases with angular frequency (follows from eqn (1)). Hence at higher temperature the pore size becomes optimal for the higher modes. This results in the growth of acoustic power in higher modes.

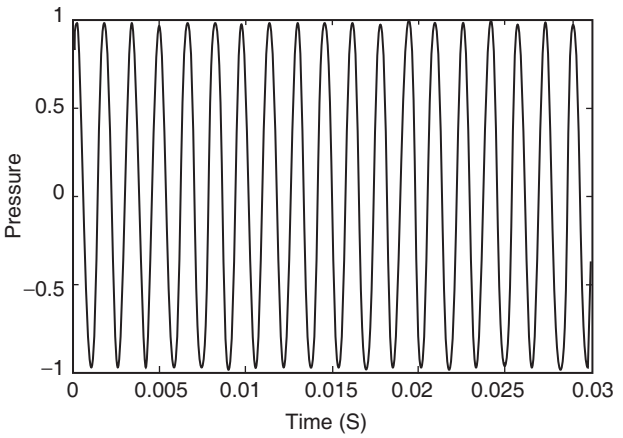

Figure 10: Time trace of acoustic pressure signal corresponding to second mode limit cycle oscillations (region IV of Fig. 3) for an input heat flux of 190 Watts. Note that all the local maxima have same amplitude. Also, the pressure values are normalized.

As the heat flux is increased further, the power in the second mode of the acoustic oscillations becomes comparable to the power in the fundamental mode. Unlike in the case of a simple duct, for the thermoacoustic engine, the second mode frequency is not an integer multiple of the fundamental mode frequency. This is due to the modification in the duct modes in presence of thermal gradient across the stack [21]. Simultaneous presence of two incommensurate frequencies results in a quasiperiodic behavior.

As the heater power is increased further, the amplitude of the fundamental mode decreases and it causes the system to lock on to a limit cycle with a frequency equal to the second resonance frequency of the resonator (3rd bifurcation). Here, it should be noted that the oscillations go from a quasiperiodic behavior to limit cycle behavior. The attractor in the phase space becomes a single loop (Fig. 12). The local maxima for the pressure trace have constant amplitude (Fig. 10) and FFT of pressure time series shows presence of singe prominent frequency (Fig. 11). This is indicative of limit cycle behavior. The absence of fundamental mode oscillations at this regime (region IV) is the result of non optimal stack pore size corresponding to the fundamental mode frequency at high stack temperature. The maximum input heat flux used for the bifurcation analysis was restricted to 250 Watts since the heater wire could not with stand power levels higher than this.

In the reverse direction of the bifurcation experiment (Fig. 3.b), it can be seen that there is a hysteresis for the first, second and third bifurcations. Hence, these bifurcations can be classified as subcritical bifurcations [18]. However, the presence of quasiperiodic oscillations in the reverse direction is limited to a single parameter location. This mismatch between forward and reverse branches of bifurcation diagram

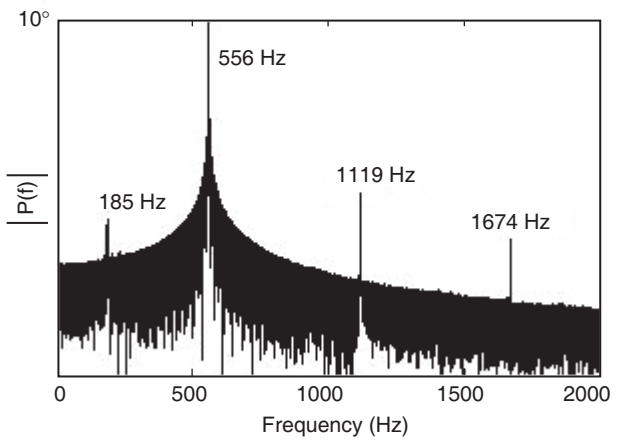

Figure 11: FFT corresponding to second mode limit cycle oscillations (region IV of Fig. 3). Here, the input heat flux is 190 Watts.

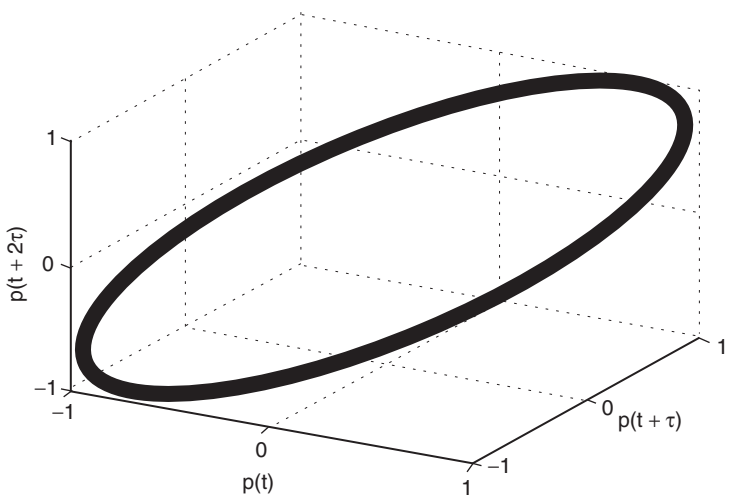

Figure 12: Phase portrait corresponding to limit cycle oscillations (region IV of Fig. 3). Here, the input heat flux is 190 Watts and the pressure values are normalized.

is indicative of the directionality of bifurcation. Atchely et al. [9] in their paper on stability analysis of multiple modes in a thermoacoustic prime mover has observed the following phenomena. In a standing wave thermoacoustic system, the presence of one mode can affect the stability of another mode. Extending this argument, in this bifurcation analysis, the direction of variation of parameter (input heat flux) becomes

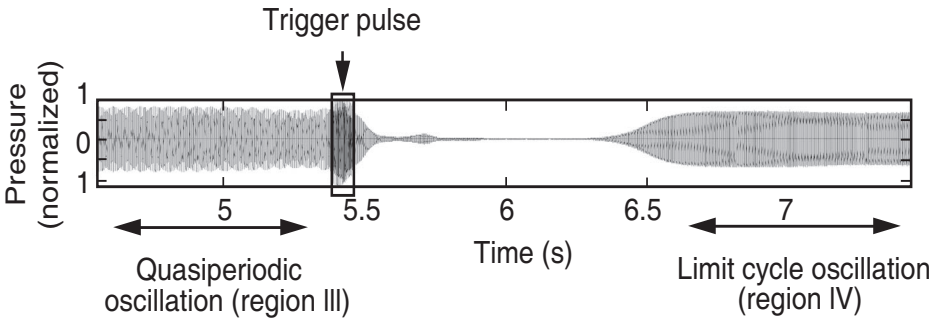

Figure 13: Transition of quasiperiodic oscillation to limit cycle oscillation through triggering. An acoustic signal (trigger pulse) was used to enable triggering. The trigger pulse was produced using an acoustic driver. The pulse had a frequency of 200 Hz, a width of 0.1*s* and an amplitude roughly 1.3 times the amplitude of self-excited oscillation.

significant in deciding the dynamic nature of thermoacoustic oscillations of the system. As the input heat flux is reduced from 250 Watts (Fig. 3.b), the onset of fundamental mode is inhibited by the presence of oscillations in second mode. This leads to a reduced quasiperiodic region (region III) in the reverse bifurcation diagram compared to the forward bifurcation diagram.

The above behavior indicates the presence of two stable attractors at the parameter locations in region III (quasiperiodic oscillation) of forward bifurcation diagram (Fig. 3.a). Hence experiments were performed to confirm their simultaneous existence. It was observed that when the system is exhibiting quasiperiodic oscillations, a trigger pulse can take the system to limit cycle oscillations corresponding to the second mode (Fig. 13). This confirms the simultaneous existence of two stable attractors in the phase space.

We saw that multiple bifurcations in oscillatory characteristics with varying input heat flux cause large fluctuations in operational frequency. As explained before, this frequency variation can cause reduction in overall efficiency of thermoacoustic generator. Hence, in order to avoid these variations, the following precautions can be adopted. One method would be to use a resonator duct with its acoustic mode widely separated in frequency (e.g. Helmholtz resonator [22]). Selecting an appropriate resonator, we can ensure that input heat flux (and hence the stack temperature) for which the higher mode oscillations will have comparable power to the first mode oscillations will be very high and out of the operational range. Further, the growth of a particular mode can be inhibited by introducing flow resistance at locations corresponding to its anti-nodes of velocity fluctuation [9]. Another design modification that will ensure larger stability zone for fundamental mode (region II) is to reduce the ratio of stack length to wave length (λ_s). It was observed from our experiments that a stack of λ_s less than 0.07 produced only fundamental mode oscillations for the given operational range of input heat flux (0 to 250 watts of input heat flux). However, the amplitude of the pressure

oscillations in this case was lower than the previous case. Using a stack with a varying pore size will be another way to avoid multiple modes. The pore size has to vary in such a way that at each location in the stack, the pore size should be optimized for local thermal penetration depth. This implies that the pore size near the hot heat exchanger has to be higher than the pore size near the cold heat exchanger. This however is difficult to achieve considering the difficulties in fabrication.

5. CONCLUSIONS

The variation in the dynamic behavior of thermoacoustic engine with varying input heat flux was explored through an experimental study. A series of bifurcations in the qualitative nature of the thermoacoustic oscillations were observed through which the system exhibited various dynamic characteristics such as fundamental mode oscillations, quasiperiodic oscillations and second mode oscillations. The hysteresis in the bifurcation diagram suggests that the bifurcations are subcritical in nature. Further, various dynamic regimes were studied using phase portrait, FFT and time trace of the pressure signal. It was seen that the interaction between multiple modes of the thermoacoustic engine with incommensurate frequencies gave rise to quasiperiodic oscillations. The simultaneous presence of two modes with incommensurate frequencies was attributed to the varying thermal penetration depth of the working fluid along the stack at different input heat flux rates. From experiments, the presence of two stable phase space attractors at the quasiperiodic regime was established. Further, some design suggestions to avoid significant variations in the oscillatory characteristics of the thermoacoustic engine were provided. However, an extensive study of dynamic characteristics of a TAE with varying operational conditions (other parameters such as stack length, position etc.) is essential in order to improve the performance of a TAE used for practical power generation applications. Further, a future study shoud also look into the energy transfer from the fundamental mode to the higher harmonic modes induced by the nonlinear effects (such as streaming effect etc.) caused by the high intensity thermal flux.

6. ACKNOWLEDGEMENT

Authors would like to acknowledge the financial support of CSIR-CEERI under Supra Institutional Project (SIP-21 activity). We would also like to acknowledge the helpful suggestions from Tobias Holzinger (TU Munich) for the construction of TAE and the support from V. Vineeth Nair (IIT Madras) for nonlinear time series analysis.

REFERENCES

[1] G. W. Swift. Thermoacoustic engines. *The Journal of the Acoustical Society of America*, 1988, 84(4):1145–1180.

[2] S. Backhaus. Initial tests of a thermoacoustic space power engine. *AIP Conference Proceedings*, 2003, 654(1):641–647.

[3] A. Alemany, Krauze A., and Radi M. A. Thermo acoustic - {MHD} electrical generator. *Energy Procedia*, 2011, 6(0):92–100.

[4] N. Rott. Thermally driven acoustic oscillations, part iii: Second-order heat flux. *Zeitschrift fur angewandte Mathematik und Physik ZAMP*, 1975, 26(1):43–49.

[5] N. Rott and Zouzoulas G. Thermally driven acoustic oscillations, part iv: Tubes with variable crosssection. *Zeitschrift fur angewandte Mathematik und Physik ZAMP*, 1976, 27(2):197–224.

[6] U. A. Muller and Rott N. Thermally driven acoustic oscillations, part vi: Excitation and power. *Zeitschrift fur angewandte Mathematik und Physik ZAMP*, 1983, 34(5):609–626.

[7] T. Yazaki, Takashima S., and Mizutani F. Complex quasiperiodic and chaotic states observed in thermally induced oscillations of gas columns. *Phys. Rev. Lett.*, Mar 1987, 58:1108–1111.

[8] L. Kabiraj, Wahi P., and Sujith R. I. Bifurcations of self-excited ducted laminar premixed flame. *Journal of Engineering for Gasturbines and Power*, 2012, 134(031502).

[9] A. A. Atchley and Kuo F. M. Stability curves for a thermoacoustic prime mover. *The Journal of the Acoustical Society of America*, 1994, 95(3):1401–1404.

[10] Z. Yu, Jaworski A. J., and Abduljalil A. S. Fishbone-like instability in a looped-tube thermoacoustic engine. *The Journal of the Acoustical Society of America*, 2010, 128(4):EL188–EL194.

[11] Z. B. Yu, Li Q., Chen X., Guo F. Z., and Xie X. J. Experimental investigation on a thermoacoustic engine having a looped tube and resonator. *Cryogenics*, August 2005, 45:566–571.

[12] T. Biwa, Y. Ueda, T. Yazaki, and U. Mizutani. Thermodynamical mode selection rule observed in thermoacoustic oscillations. *EPL (Europhysics Letters)*, 2002, 60(3):363.

[13] H. XingHua, Qing Z. X., and Ling W. H.and Ming S. S. Two-port network model and startup criteria for thermoacoustic oscillators. *Chinese Science Bulletin*, 2009, 54(2):335.

[14] H. Yuan, Karpov S., and Prosperetti A. A simplified model for linear and nonlinear processes in thermoacoustic prime movers. part ii. nonlinear oscillations. *The Journal of the Acoustical Society of America*, 1997, 102(6):3497–3506.

[15] B. Ward and Clark J.and Swift G. W. *Design Environment for Low-amplitude Thermoacoustic Energy Conversion*. Los Alamos National Laboratory, version 6.2 edition, 2008. Available from: www.lanl.gov/thermoacoustics/DeltaEC.html.

[16] H. D. I. Abarbanel. *Analysis of observed chaotic data*. Springer-Verlag, New York, 1996.

[17] F. Takens. In dynamical systems and turbulence. Warwick 1980, edited by D.Rand and L.S.Young, 1981. Lecture note in mathematics No.898 (springer, Berlin), pp. 366.

[18] S. H. Strogatz. *Nonlinear Dynamics and Chaos: With Applications to Physics, Biology, Chemistry, and Engineering*. Levant Books, Kolkata, India, 2007.

[19] A. H. Nayfeh and Balachandran B. *Applied Nonlinear Dynamics: Analytical, Computational, and Experimental Methods*. Wiley-VCH Verlag GmbH & Co.KGaA, Weinheim, Germany, 2004.

[20] F. C. Moon. *Nonlinear Chaotic and Fractal Dynamics: An Introduction for Applied Scientists and Engineers*. Wiley-VCH Verlag GmbH &Co.KGaA, Weinheim, Germany, 2004.

[21] R. I. Sujith, Waldherr G. A., and Zinn B. T. An exact solution for one-dimensional acoustic fields in ducts with an axial temperature gradient. *Journal of Sound and Vibration*, 1995, 184(3):389–402.

[22] L. E. Kinsler and Fray L. *Fundamentals of Acoustics*. 1999.